ELSEVIER

Journal of Molecular Catalysis A: Chemical 96 (1995) 65–75

JOURNAL OF MOLECULAR CATALYSIS A: CHEMICAL

Catalytic and structural properties of ruthenium monometallic and bimetallic catalysts: characterization by EXAFS and XRD

M. Concepción Sanchez Sierra *, Joaquin García Ruiz, M. Grazia Proietti, Javier Blasco

ICMA, CSIC – Universidad de Zaragoza, Facultad de Ciencias, Pza. S.Francisco s.n., 50009 Zaragoza, Spain

Received 28 June 1994; accepted 7 October 1994

Abstract

This work presents an extensive structural study of Ru monometallic (Ru/Al_2O_3) and bimetallic (RuM/Al_2O_3, M = Ge, Sn, Pb) catalysts by means of extended X-ray absorption fine structure (EXAFS) at the Ru K-edge, and X-ray powder diffraction. Samples prepared by the controlled surface reaction (CSR) technique and by the classical impregnation method with different Ru loadings and different Ru/M weight ratios were studied. The results show that monometallic catalysts contain small Ru clusters whose degree of dispersion, measured from the average Ru coordination numbers, decreases with the Ru loading. The clusters are formed by metallic ruthenium. The Ru 1% weight sample, prepared by the controlled surface reaction technique, is the most highly dispersed, comprising small clusters of no more than 12 atoms. The samples prepared by this latter technique are in general better dispersed than those prepared by the impregnation method. Addition of germanium produces an increase of Ru dispersion, and in the case of the highest Ge/Ru ratio, bimetallic clusters formed. The degree of dispersion is higher in some Sn-containing catalysts while lead does not induce any structural change.

Keywords: Bimetallic catalysts; Monometallic catalysts; Ruthenium; Structural properties; XRD

1. Introduction

This paper is part of a series which describes the studies performed on ruthenium based catalysts and we refer to the first paper of the series for a detailed exposition of the general objectives to be covered [1].

The general scope of this work is to correlate the structural and catalytic properties of model ruthenium catalysts alloyed with Sn, Pb, Ge and prepared by means of the controlled surface reaction (CSR) technique [2]. In this method, starting from the same monometallic 'parent catalyst', different bimetallic formulations were prepared by adding different amounts of the second element. Catalysts prepared by the classical coimpregnation method were also studied.

The effect of dispersion on the catalytic properties of Ru monometallic catalysts has been well established, as hydrogenolysis and isomerization of alkanes, the product selectivities and their alteration with H_2 pressure change with the degree of dispersion and pretreatment used [3–5].

In the case of bimetallic RuM particles several works on the hydrogenolysis of alkanes have suggested that Sn and Pb atoms occupy specific sites of low coordination numbers, whereas Ge has not so definite a preference [6–8]. The modifiers

* Corresponding author.

SSDI 1381-1169(94)00022-0

induce a lowering of the Ru activity for structure-sensitive reactions, as for example alkane hydrogenolysis, as well as changes related to chemisorption mechanism of the reactant alkane molecules [6]. Analogous changes are also observed with the hydrogenation of polyfunctional molecules [9].

Since a better knowledge of the basic phenomena responsible for the improvement of the catalytic activity is needed, we have performed a systematic investigation of the monometallic and bimetallic catalysts by means of the extended X-ray absorption fine structure (EXAFS) technique [10] that is well known to provide detailed structural information concerning short-range order on a wide range of materials. The knowledge of the Ru local environment could solve indeed several critical questions concerning the structural properties of these systems. For example, are the two metals present in the same aggregates? What is the ratio between surface and bulk ruthenium atoms?

This work deals with the structural characterization, using EXAFS spectroscopy at the Ru K edge, of several Ru based monometallic and bimetallic catalysts supported on alumina. We present a comparative study of Ru monometallic catalysts, with different Ru loadings, prepared following the two preparative procedures, and of the effect on the local structure around the Ru atoms when modifiers such as Ge, Pb and Sn are added. X-ray powder diffraction (XRD) experiments were also performed on some selected samples.

Caracterization of monometallic Ru catalysts by EXAFS was performed in the past [11] and bimetallic Ru–Cu catalysts were studied by Sinfelt [12].

Nevertheless a systematic comparative investigation at different Ru loadings and different preparative procedures has not been reported yet. Moreover, the use of the same parent sample for the bimetallic formulations allows direct determination of the influence of the different modifiers on the Ru particles.

The preparation of monometallic and bimetallic Ru catalysts by means of the CSR, using organometallic precursors, and their characterization, was performed at the Montpellier University [1]. Catalysts prepared by the classical impregnation method were made at Messina University [1]. The distribution of the added modifier were investigated by means of 2,2,3,3-tetramethylbutane (TeMB) hydrogenolysis [7], IR spectroscopy of absorbed CO and quantum chemical calculations of model bimetallic clusters[13]. Moreover, hydrogenation of unsaturated compounds in the gas and liquid phase [14] and physical characterization by XPS and TEM were also perfomed [1].

2. Experimental

2.1. Preparation of catalysts

The catalysts from organic precursors (RuEC series) were prepared from γ-Al_2O_3 and ruthenium acetylacetonate $Ru(acac)_3$, by ligand exchange according to procedures described by Boitiaux et al. for Pd/Al_2O_3 catalysts [15]. After the ligand exchange was completed the solution was filtered to obtain well dispersed catalysts (RuEC1 sample), or evaporated to get a medium dispersion (RuEC2 and RuEC3 samples). The monometallic catalysts were used as a basis for the bimetallic formulations. The second metal was introduced as a tetra-n-butyl tin, tetraethyl lead or tetra-n-butyl germanium. The bimetallic RuM/Al_2O_3 (M = Ge, Sn, Pb) formulations were prepared by contacting 'in situ' the Ru/Al_2O_3 parent catalyst, prereduced at 623 K, with the different required amounts of tetra-alkyl-M in n-heptane solution. The controlled surface reaction was carried out under H_2 atmosphere at 333 K with a solid/liquid ratio of 1 g/3 cm^3 [1].

The preparation of catalysts from inorganic precursors was carried out at the Messina University. Ruthenium nitrosyl nitrate (RuNI series) and ruthenium trichloride (RuCI sample) were used as precursors. The bimetallic samples were made by simultaneous impregnation of the Al_2O_3 with ruthenium nitrosyl nitrate and germanium ethoxide, $SnCl_2$, lead acetate and $SnSO_4$ in order to add,

Table 1
Composition and chemisorption characteristics of the Ru catalysts (from [1]): Ge, Sn, Pb and Ru weight percentages (wt.%), total H_2 chemisorption as ratio between H_2 chemisorbed and Ru content $(H/Ru)_{tot}$, irreversible H_2 chemisorption $((H/Ru)_{irr})$, CO chemisorption as ratio between CO chemisorbed and Ru content (CO/Ru)

Sample	Ge, Sn, Pb (wt.%)	Ru (wt.%)	$(H/Ru)_{tot}$	$(H/Ru)_{irr}$	CO/Ru
RuEC1	–	0.97	0.88	0.71	1.31
RuEC2	–	2.5	0.44	0.38	0.64
RuEC3	–	4.0	0.25	0.19	0.27
RuEC1Ge1	0.15	0.97	0.59	0.43	1.18
RuEC1Ge2	0.30	0.97	0.54	0.38	1.21
RuEC1Ge3	0.70	0.97	0.41	0.27	1.17
RuEC1Sn1	0.2	0.97	0.51	0.37	0.86
RuEC1Pb1	0.2	0.97	0.66	0.53	1.30
RuEC3Fe1	0.41	4.0	0.12	–	–
RuNI1	–	1.0	0.23	0.17	0.37
RuNI2	–	2.0	0.23	0.17	0.31
RuNI4	–	4.0	0.26	0.20	0.30
RuNIGe1	0.14	1.0	0.59	0.45	1.07
RuNIGe2	0.20	1.0	0.54	0.40	1.03
RuNIGe3	0.72	1.0	0.42	0.28	1.04
RuNI1Sn1	0.23	1.0	0.38	0.26	0.98
$RuNI1SnSO_4$	0.23	1.0	0.25	0.18	0.79
RuNI1Pb	0.41	1.0	0.36	0.27	0.83
RuC1	–	1.0	0.22	0.12	0.20

as a second metal, Ge, Sn, and Pb respectively.

A detailed description of these preparative procedures has been reported elsewhere [1] and a list of the catalysts, with their Ru content and results on chemisorption uptake for hydrogen and carbon monoxide, is reported in Table 1.

2.2. EXAFS and XRD

X-ray absorption experiments at the Ru K-edge were carried out at the beam line XAS IV of the storage ring DCI of LURE (Laboratoire pour l'Utilisation de la Radiation Electromagnetique) at Orsay. A double crystal Si(311) monochromator was used and the storage ring operated at 1.8 GeV with an average current of 150 mA.

The experiments were performed at room temperature in the transmission mode and the samples were mounted into a special chamber to be reduced 'in situ'. The catalysts were measured before and after reduction by flowing hydrogen at

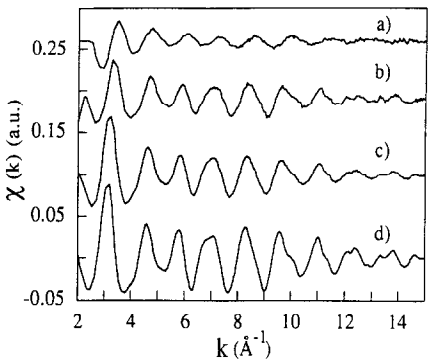

Fig. 1. Ru K-edge raw EXAFS spectra of RuEC catalysts series (from a to c) and of metallic Ru (curve d). The origin of the vertical axis refers to curve d, the other curves have been shifted upwards for sake of clarity.

450°C for one hour. The EXAFS spectra of the 'as received' samples show partial or total oxidation of the ruthenium clusters. The reduction process was monitorized by EXAFS while sample homogeneity and optimal thickness were tested in advance by means of the laboratory EXAFS spectrometer of the 'Servicio Nacional de EXAFS de la Universidad de Zaragoza'. The precursor $Ru(acac)_3/Al_2O_3$ and metallic ruthenium (Ru^0) were also measured for use as reference.

The experimental EXAFS signals were extracted from the raw spectra by using standard techniques [10]. The atomic-like term $\mu_0(E)$ was determined by a cubic spline approximation. The EXAFS signal was determined as $\chi(k) = \mu(k) - \mu_0(k)/\mu_0(k)$, where the photoelectron wave vector is given by $k = (2m(E-E_0))^{1/2}/\hbar$. E_0 is the photoelectron binding energy taken as the energy at the inflexion point of the absorption edge. The raw EXAFS spectra of the RuEC series are reported in Fig. 1, together with the spectrum of metallic Ru, as an example of data quality. An analogous spectrum quality was obtained for the other samples. The k^2-weighted spectra were then Fourier transormed from k to R space in the range 3.4–14 $Å^{-1}$ after being multiplied for a Hanning window with an apodization value of 0.2 $Å^{-1}$. The relationship between $\chi(k)$ and the structural parameter is given by the well known EXAFS formula [10]:

$$\chi(k) = \Sigma_i 1/k(N_i/R_i^2)e^{-2R_i/\lambda(k)} e^{-2\sigma^2 k^2} F_i(k)\sin[2kR_i + \Phi_i(k)] \quad (1)$$

where the subscript i refers to the ith coordination shell, R_i is the interatomic absorber–scatterer distance, N_i is the number of atoms of the ith shell, σ_i is the Debye–Waller factor, $F_i(k)$ and $\Phi_i(k)$ are the amplitude backscattering function and phase shift respectively, and λ is the photoelectron mean free path.

The first shell contribution was extracted by Fourier-filtering the FT spectra between 1.2 and 3 Å and the corresponding structural parameters have been obtained by least squares fitting of the filtered k-weighted spectrum with Eq. 1 ($i=1$). Backscattering amplitudes and phase shifts were obtained from Ru^0 and $Ru(acac)_3$ EXAFS for the Ru–Ru and Ru–O pairs, respectively. For the Ru–Ge contribution instead, theoretical phases and amplitudes, generated from the FEFF3.11 code [16], were used because of the lack of proper reference samples. We emphasize that the Fourier analysis as well as the best fit procedure have been carried out in the same way and with the same parameters for the whole set of samples to avoid any possible analysis artifacts.

X-ray diffraction experiments have been carried out at the University of Zaragoza using a Cu rotating anode generator as a source. The diffracted beam was monochromatized by a graphite crystal. The diffractograms were performed, at room temperature, on air-exposed samples.

3. Results

3.1. Monometallic catalysts

The Fourier transform (FT) of the Ru K EXAFS spectra of monometallic catalysts have been plotted in Fig. 2 and compared with that of metallic Ru. The FT of the whole series is characterized by a main peak which lies at the same position as that of Ru^0. For samples with higher Ru loadings the FT structures at higher R-values

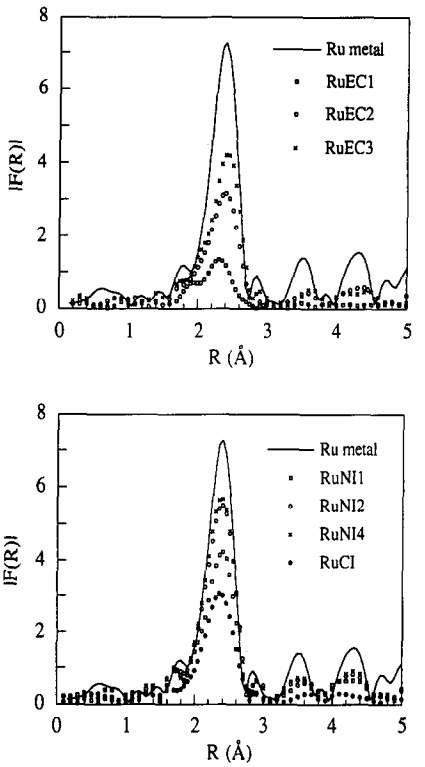

Fig. 2. Fourier transform modulus of the K Ru edge EXAFS spectra of monometalllic Ru catalysts with different Ru loadings compared with that of metallic Ru. Upper panel: catalysts prepared by the CSR technique. Lower panel: catalysts prepared by classical impregnation method.

are very similar, also if with a lower intensity, with those showed by Ru^0. These results show that the catalyst is formed, as expected, by small Ru particles. The height of the main peak increases with the Ru loading for the same preparative method and for the RuNI series is larger than for the RuEC series.

The first shell contribution has been analyzed by curve fitting of the Fourier filtered spectra to the EXAFS Eq. 1. For illustration the comparison between the experimental and the fitted EXAFS for some selected samples is shown in Fig. 3. The best fit values for the Ru–Ru interatomic distances, coordination numbers and Debye–Waller factors (reported as difference with Ru^0) of the monometallic catalyst are summarized in Table 2. The errors on the fit parameters were evaluated by changing each variable, while refining the others,

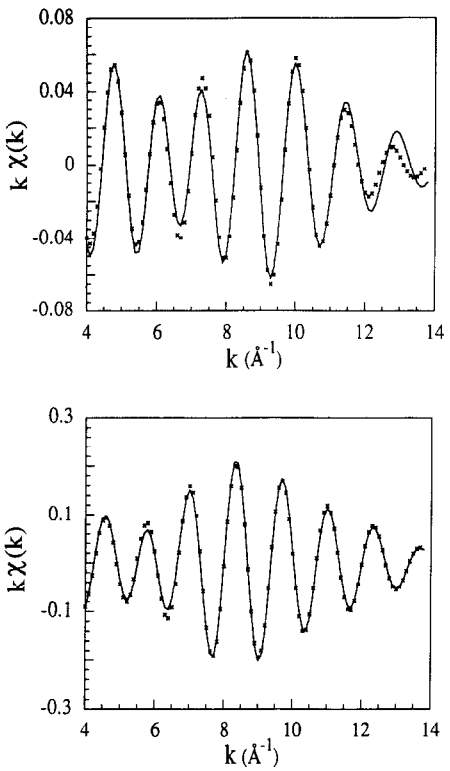

Fig. 3. Experimental k^3-weighted first shell filtered spectra of Ru (Ru 1%) monometallic catalysts (——) with the best fit simulation (× ×). Upper panel: RuEC1 catalyst; lower panel: RuNI1 catalysts.

until the residual at minimum was doubled [17]. The error bar on the coordination numbers is about 10% for the Ru^0–Ru^0 coordination shell and grows up to 50% for the less important first shell contributions as the Ru^0–$Ru^{\delta+}$ and Ru^0–O shells. The errors on the Debye–Waller factors are of about 0.002 Å^2 in all the cases. The sensitivity on bond length changes is instead quite better and the errors on the R values are of 0.01 Å for the Ru^0–Ru^0 bond length and of 0.04 Å for the Ru^0–$Ru^{\delta+}$ and Ru^0–O distances. The same error values are found for the whole set of samples being the data quality similar and the analysis carried out in the same way for each of them.

As can be observed, Ru is always coordinated only with Ru at a distance of 2.67 Å that is equal to the metal Ru^0–Ru^0 bond length. A slightly shorter distance of 2.60 Å is observed in the RuEC1 sample. This bond length contraction is in agreement with quantum chemical calculations performed on Ru_9 model clusters having an average diameter of less than 9 Å [13]. The coordination numbers increase with the Ru loading for each kind of preparation and, for the same loading, the catalysts prepared by the CSR method are more dispersed, showing coordination numbers lower than those prepared by the classical impregnation method. For the lowest Ru loading, the RuEC1 sample, a shorter Ru–Ru distance of about 2 Å is also observed. It is indicated in Table 2 as $Ru^{\delta+}$ and is observed together with the presence of oxygen atoms at about the same distance. The presence of the shorter Ru–$Ru^{\delta+}$ bonds has already been observed by Vlaic et al. [11] and its origin is still unclear. It can be related to the presence of an oxygen coordination shell that may be due to the higher dispersion of the Ru particles establishing a closer contact with the oxygen atoms of the support, as well as to a less efficient reduction of the catalyst.

X-ray diffraction patterns of the highest Ru content catalysts show small peaks which correspond to reflections from crystalline Ru^0 superimposed to the much more intense X-ray pattern from Al_2O_3. The XRD diagrams of the RuEC series and

Table 2
Best fit parameters obtained for the first shell contribution of monometallic catalysts (N: coordination numbers, R: distance from the Ru absorber, $\Delta\sigma^2$: Debye–Waller factors difference between catalysts and reference compound), and particle size, in Å, obtained by X-ray diffraction. The errors on the fit parameters, not reported in the table for the sake of brevity, are (see also text): $\Delta N_{Ru^0}/N_{Ru^0} \cong 10\%$, $\Delta N_{Ru^{\delta+}}/N_{Ru^{\delta+}} \cong \Delta N_{Ru^{\delta+}}/N_{Ru^{\delta+}} \cong 50\%$, $\Delta R_{Ru^0} = \pm 0.01$Å, $\Delta R_{Ru^{\delta+}} = R_O = \pm 0.04$, $\Delta\sigma^2 = 0.002$ Å^2

Sample	N		R (Å)	$\Delta\sigma^2$(Å)	d_{XRD} (Å)
metallic Ru	Ru^0	12	2.66	0.00	>1000
RuEC1	Ru^0	3.8	2.60	0.003	no metallic Ru detected
	$Ru^{\delta+}$	0.5	1.99	0.002	
	O	0.3	2.02	0.002	
RuEC2	Ru^0	7.4	2.67	0.001	<20
RuEC3	Ru^0	9.9	2.67	0.002	<25
RuNI1	Ru^0	9.2	2.67	0.001	<25
RuNI2	Ru^0	10.9	2.67	0.000	<90
RuNI4	Ru^0	11.2	2.67	0.000	<80
RuC1	Ru^0	10.4	2.65	0.000	no metallic Ru detected

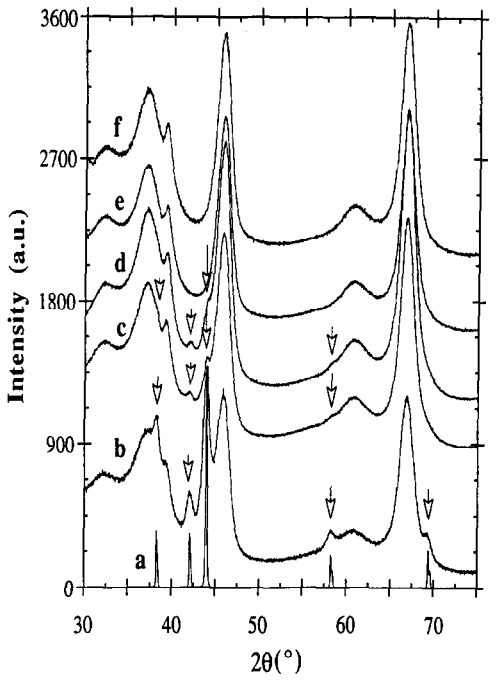

Fig. 4. XRD patterns of the RUEC and RuNI2 catalysts compared with metallic Ru and Al_2O_3: (a) metallic Ru; (b) RuNI2; (c) RuEC1; (d) RuEC2; (e) RuEC3; (f) Al_2O_3. Peaks corresponding to reflections from metallic Ru, indicated by the arrows, appear for all the catalysts except for the RuEC1 sample.

RuNI2 sample compared with that of metallic ruthenium are shown in Fig. 4. The particle size has been estimated by using the Scherrer equation and the values obtained are reported in Table 2. No diffraction peaks from Ru have been observed in the RuEC1 and RuCl catalysts.

On the basis of the EXAFS and XRD results we can therefore deduce that, for the Ru-richest samples, the catalysts consist of small particles of Ru^0 whose dispersion depends on the Ru content. In the case of RuEC1 catalysts is more difficult to establish the sample morphology and we will discuss this subject again later.

3.2. *Bimetallic catalysts*

The FT of the EXAFS spectra of Ru–Ge/Al_2O_3 catalysts are shown in Fig. 5. No appreciable modification is observed between RuEC3Ge1 sample and the parent RuEC3 sample, indicating that the particle size remains unaltered after Ge addition.

In the case of lower Ru content, i.e., the RuEC1 derived samples, germanium addition induces a decrease of the component of the FT spectra having higher R-values, corresponding to the Ru–Ru coordination shell contribution, and an increase of the lower R-contribution to the FT peak, related to the Ru–O pairs. This means that the material is more oxidised and dispersed. The addition of Ge to the RuNI samples induces instead a reduction in the intensity of the main peak (see Fig. 6) without any modification of the distance, indicating a decrease of Ru coordination.

The EXAFS spectra of the bimetallic Sn–Ru and Pb–Ru catalysts are very similar to the monometallic parent samples, both for samples prepared by the CSR tecnhique and for those prepared by the classical impregnation method. The only exception is the RuNISn sample obtained from $SnCl_2$ impregnation, which shows a large reduction of the EXAFS amplitude. A small increase of

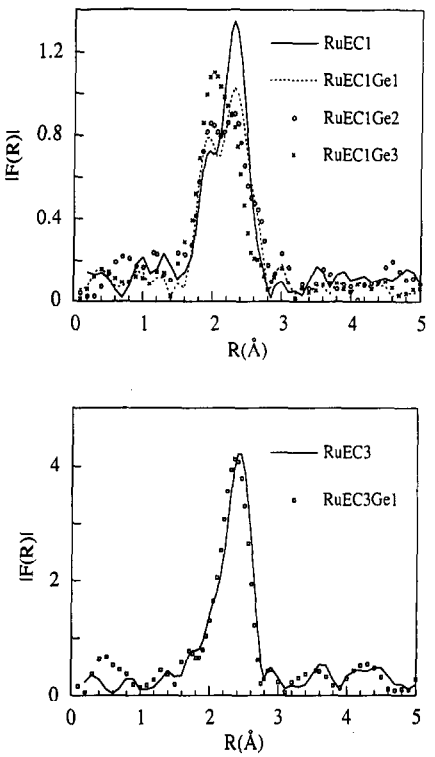

Fig. 5. Fourier transform of the EXAFS spectra of bimetallic RuEC1Ge catalysts at different Ru/Ge ratios, compared with the monometallic parent catalyst RuEC1. An evident modification of the main peak occurs upon Ge addition.

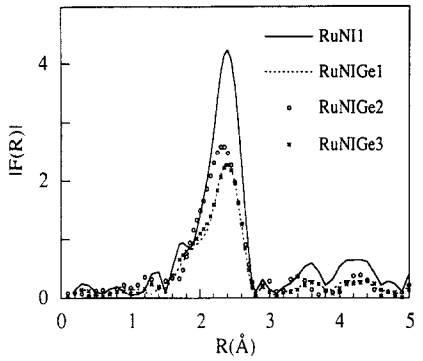

Fig. 6. Fourier transform of the EXAFS spectra of bimetallic RuNIGe catalysts with different Ru/Ge ratio compared with the monometallic parent catalyst RuNI. Germanium addition induces a lowering of the main peak indicating a more dispersed catalyst.

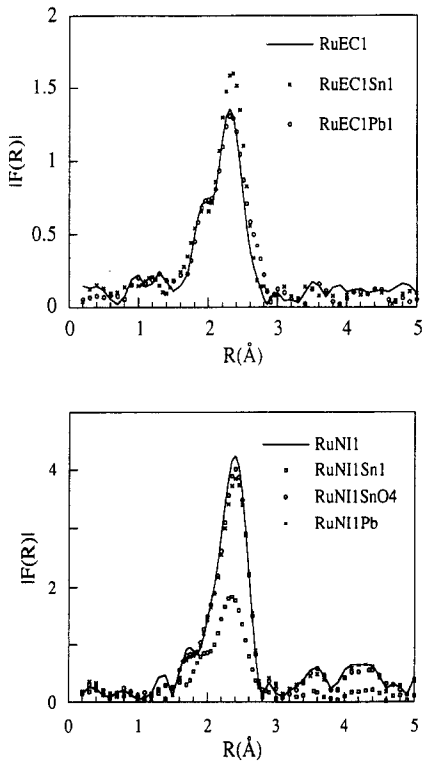

Fig. 7. Fourier transform of the EXAFS spectra of bimetallic Ru/Sn and Ru/Pb catalysts compared with the monometallic parent catalyst. Upper panel: catalysts prepared by the CSR technique. Lower panel: catalyst prepared by the classical impregnation method.

the coordination numbers of Ru^0 and $Ru^{\delta+}$ is observed for the RuEC1Sn1 sample but it cannot be regarded as very significant. The comparison of the FT for the two series is given in Fig. 7.

The first shell structural parameters for bimetallic catalysts were obtained by the same procedure employed for the monometallic samples, i.e. by curve fitting of the Fourier filtered EXAFS data, and the best fit results are given in Table 3. In the case of the RuEC1Ge3 sample, for which four shells of contribution are reported, the Ru^0–Ru^0 and the Ru^0–$Ru^{\delta+}$ distances, as well as the $\Delta\sigma^2$ of the Ru–O pair, have been left fixed during the fit and put equal to the values found for the monometallic parent catalyst. It is reasonable from a physical point of view and, at the same time allows us, in terms of fit allowed variables, to introduce a further coordination shell in the least square minimization process. The errors have been evaluated as described in the previous section and similar values were found (see caption Table 3).

Table 3
Best fit parameters obtained for the first shell contribution of bimetallic catalysts. N: coordination numbers, R: distance from the Ru absorber, $\Delta\sigma^2$: Debye–Waller factors difference between catalysts and metallic Ru. The errors on the fit parameters are the same as those reported for the monometallic catalysts (Table 2). For the Ru–Ge pair the errors are: $\Delta N_{Ru-Ge}/N_{Ru-Ge} \cong 50\%$, $R_{Ru-Ge} = \pm 0.01$Å, $\Delta R_{Ru-Ge} = \pm 0.04$, $\Delta\sigma^2 = 0.002$ Å^2

Sample		N	R (Å)	$\Delta\sigma^2$ (Å^2)
metallic Ru	Ru^0	12	2.66	0.00
RuEC1Ge1	Ru^0	3.4	2.62	0.003
	$Ru^{\delta+}$	0.5	1.95	0.002
	O	0.3	2.01	0.002
RuEC1Ge2	Ru^0	3.1	2.62	0.003
	$Ru^{\delta+}$	0.5	1.95	0.002
	O	0.5	1.98	0.002
RuEC1Ge3	Ru^0	2.0	2.62	0.007
	$Ru^{\delta+}$	0.5	1.96	0.003
	O	0.6	2.01	0.002
	Ge	1.8	2.45	0.004
RuEC3Ge1	Ru^0	9.8	2.66	0.002
RuEC1Sn1	Ru^0	4.6	2.63	0.003
	$Ru^{\delta+}$	0.9	1.99	0.002
	O	0.3	2.02	0.002
RuEC1Pb1	same best fit parameters as parent monometallic RuEC1, no Pb detected			
RuNIGe1	Ru^0	6.1	2.66	0.002
RuNIGe2	Ru^0	6.4	2.65	0.001
RuNIGe3	Ru^0	6.0	2.66	0.002
RuNI1Sn1	Ru^0	6.0	2.66	0.001
$RuNI1SnSO_4$	Ru^0	10.4	2.65	0.000
RuNIPb1	same best fit parameters as parent monometallic RuNI1, no Pb detected			

Ge addition to the RuEC1 samples produces a decrease of the metallic Ru^0–Ru^0 coordination: the higher the Ge content the lower the coordination number. It is the other way round for O, whose coordination numbers increase, as the FT spectra already suggested, with the Ge content. For the RuEC1Ge samples a Ru^0–$Ru^{\delta+}$ contribution to the first coordination sphere is observed showing distance and coordination number values similar to those of the parent monometallic catalyst. It seems to be related, as mentioned before, to the higher Ru dispersion and/or to a less efficient reduction of the sample and does not vary with the loading of the second metal.

For the sample RuEC1Ge3, with the highest Ge concentration, the best fit results suggest, as the only case in the whole bimetallic series, the presence of the second metal in the first coordination shell of Ru, meaning the incorporation of a small amount of Ge in the Ru particles.

When Pb is added to the RuEC1 catalysts no changes in the coordination numbers, and as a consequence in the degree of dispersion, are observed. A slight increase of the Ru^0 coordination numbers is observed upon adding Sn but neither Pb nor Sn are in any case detected in the Ru first coordination shell.

The best fit results on the RuNI1 series, prepared also by adding Ge and Sn, show a decrease of the Ru coordination number, pointing to an increasing dispersion, for the Ge-doped sample and for the sample obtained by $SnCl_2$ impregnation. For the other Sn (RuNI1$SnSO_4$) and Pb containing samples, the best fit is obtained with the same parameters as used for the monometallic samples, indicating that no modification of the average local structure around Ru occurs, in agreement with the qualitative considerations on the FT spectra comparison.

4. Discussion

The EXAFS study performed on the Ru monometallic catalysts shows that the coordination numbers increase with Ru loading, indicating an increase of the Ru particle size. The dispersion of catalysts prepared by the CSR technique is higher for the same Ru content than those prepared by the classical impregnation method. The EXAFS signal of the highest Ru content catalysts, together with its FT, shows almost the same oscillatory behaviour and the same R-peaks as Ru^0 indicating that the Ru local environment in the catalyst is very similar to that of Ru (see Figs. 1 and 2). The particle size, obtained from the XRD data tends in general to rise with Ru loading, being about 20–25 Å in the RuEC2 and RUEC3 samples and changing from 25 up to 90 Å in the RuNI series.

In order to formulate some structural modeling of Ru in the catalyst, we tried to establish some link between coordination number and particle size. We have calculated the average coordination number of different ruthenium clusters, taking as a model the hexagonal close packing of the Ru^0 structure. Due to the fact that Ru is highly coordinated in the metallic phase, $N=12$, small changes in coordination implies large reductions of the particle size. As an example, for an infinite monolayer the coordination is already 6. Considering instead a hexagonal cluster composed by 13 atoms (see Fig. 8a), $N=5.5$ is obtained, 12 atoms

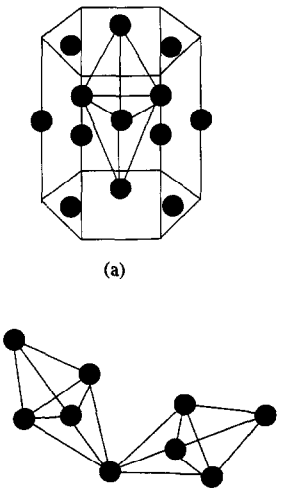

Fig. 8. (a) Ru cluster composed by 13 atoms, derived from the hcp structure of metallic ruthenium, a bipyramidal unit is shown; (b) two bipyramidal units linked randomly to each other.

out of the 13 belonging to the cluster, being surface atoms. If we increase the cluster size and make an average of different possible geometries, we obtain that for a cluster of 50 atoms $N=7.2$, for 100 atoms $N=8.1$, for 300 atoms $N=9.2$, for 500 atoms $N=10$ and so on. We can conclude therefore that for samples with coordination numbers lower than 5 all the atoms in the clusters should be surface atom with the result that it is very difficult to establish the cluster morphology and allows us only to say that for the RuEC1 sample the average cluster would be formed of no more than 12 atoms. The absence of a second shell contribution as well suggests that this system could be characterized by a non-compact cluster structure built up starting for example from the basic cell of Ru^0. In Fig. 8a we show a possible bipyramidal cluster, formed by 5 atoms, originated from the hexagonal-close-packed structure of metallic Ru. The average coordination number is $N=3.6$, which is near to the values observed for RuEC1and suggests that the highly dispersed RuEC1 catalyst could be formed by small Ru clusters with tetrahedral/bipyramidal building units deriving from the hcp structure of Ru^0 and linked randomly to each other in an amorphous and inhomogeneous phase (see Fig. 8b). The atoms of the bipyramids would have a coordination number of three or four while the atoms linking different bipyramids units could show higher coordination number values.

The effect of addition of a second metal to the Ru catalyst is unclear: it produces in some cases no appreciable effect while it induces in other cases a higher dispersion and/or a higher oxidation of the Ru particles. Moreover the second metal is not easily incorporated in the Ru particles. The only case in which Ru is observed to be coordinated with the second metal is the RuEC1 sample for the highest Ge/Ru ratio. Ge seems to have in general more structural impact than tin and lead when added to the catalyst.

The results obtained from EXAFS can be summarized as follows for the two different sets of the studied samples.

4.1. RuEC1 derived samples

(i) The addition of Ge produces appreciable morphological changes as can be observed from the comparison of the FT spectra of the Ge-containing samples with the FT of the parent monometallic catalyst (see Fig. 5). The best fit results, reported in Table 3, show that the coordination numbers of the Ru–Ru pairs decrease upon adding Ge while the coordination numbers of the Ru–O pairs increase. This indicates a more dispersed and oxidised material. For the highest Ge loading a small number of Ge atoms are incorporated to the Ru particles.

(ii) The addition of Pb and Sn does not induce any appreciable variation in the local-order structures.

4.2. RuNI derived samples

(i) The effect of Ge addition, as shown in Fig. 6 is an evident decrease of the FT peak intensity without, in this case, any shape modification. The best fit results show a decrease of the first shell coordination numbers that is nearly equal for the three different Ge loadings.

(ii) The addition of Sn produces some change only in the $SnCl_2$ impregnated sample, whose Ru coordination numbers suffers a strong reduction. The rest of the Sn and Pb-containing samples do not show changes of the Ru local environment.

We can therefore say that the main result of the present work is that both Ru monometallic and ruthenium bimetallic catalysts are formed by small aggregates of Ru, and their properties seem to be related to the dispersion degree.

The particle size determined by XRD is qualitatively well correlated with the TEM observations while the particle sizes obtained from EXAFS are lower than those observed by TEM. Nevertheless we should note that TEM observations are performed on air-exposed catalysts and that, the particles being partially or totally oxidised, the particle size could considerably change.

The average coordination number of Ru can give a direct measurement of the degree of dis-

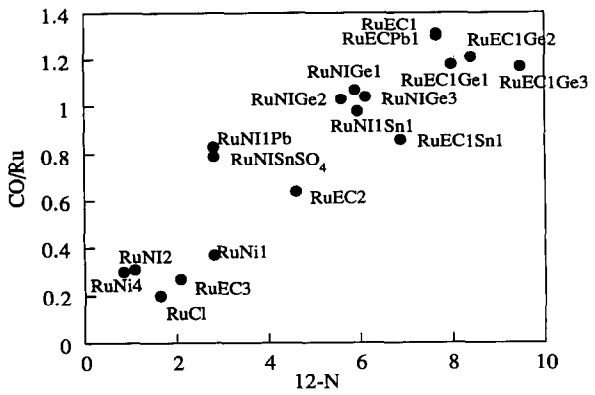

Fig. 9. CO adsorption versus free bonds, i.e., coordination of metallic Ru minus experimental coordination $(12-N)$, for all the catalysts studied.

persion and it can be correlated with chemisorption results. The H_2 and CO adsorption is larger for the RuEC series than for RuNI samples, and for the same series the increase of Ru content corresponds to an increase of the coordination number and to a decrease of H_2 and CO adsorption. The Ru–Ru average coordination versus CO adsorption is represented in Fig. 9 for all the catalysts studied. As we can observe a general dependence exists between adsorption capacity and coordination number: the lower the coordination number, the higher the CO adsorption. Only the two less dispersed catalysts deviate from the trend. It may be due to the lack of a direct correlation between average coordination and free bonds, i.e., large particles giving the same average coordination number can present different ratios of bulk/active surface. For the bimetallic catalysts CO adsorption correlates well with Ru particle size for the samples RuNISn, RuNIGe3, RuNIGe1 and RuEC1Pb, the exceptions from the trend being $RuNISnSO_4$ and RuNIPb. In more detail, for the RuNI derived samples the coordination does not change but an increase of the CO adsorption is observed, while RuEC1Sn1 behaves the other way round. It is not easy to justify all the different adsorptive types of behavior of these quite complicated systems. EXAFS experiments at tin and lead edges could give more information on the subject.

To conclude, we report structural results on a series of monometallic and bimetallic Ru-based catalysts. They indicate that for monometallic particles the main parameter which controls the adsorptive properties of the system is the degree of dispersion that is proportional to the Ru EXAFS coordination number. It depends esentially on the Ru loading and preparative procedure. Bimetallic particles are not formed except for the case of sample RuEC1Ge3. The effect of Ge addition is a lowering of the Ru particle size in all the cases studied. Similar results are obtained in some cases for Sn while Pb does not induce any modification with respect to the parent compound.

Further EXAFS experiments at the Ge, Sn and Pb K-edges are planned in order to determine the local structure around the second metal.

Acknowledgements

This work has been carried out under the auspices of the EU funded 'Stimulation Action' programme SC1-CT91-0681. We thank also the EU Large Installation programme which provided access and travel support for the experiments at LURE. We are also grateful to the LURE staff for technical assistance with special regard to Drs. D. Bazin and F. Villain for their kind help during the measurements. Thanks are also due to Prof. G.C. Bond, Prof. B. Coq and Prof. R.S. Galvagno for valuable discussions. We thank Prof. G.C. Bond also for critical reading of the manuscript.

References

[1] B. Coq, E. Crabb, M. Warawdekar, G.C. Bond, J.C. Slaa, S. Calvagno, L. Mercadante, J. García-Ruiz, M.C. Sanchez Sierra, J. Mol. Catal., 92 (1994) 107.
[2] C. Travers, T.D. Chan, R. Snappes and J.P. Bournonville, US Pat. 4,456,775 (1984).
[3] B. Coq, A. Bittar and F. Figueras, Appl. Catal., 59 (1990) 103.
[4] G.C. Bond, R. Yahya and B. Coq, J. Chem. Soc., Faraday Trans. (1990) 2297.
[5] G.C. Bond and J.C. Slaa, J. Mol Catal., 89 (1994) 221.
[6] G.C. Bond and M.R. Gelsthorpe, J. Chem. Soc., Faraday Trans. I, 85 (1989) 3767.

[7] B. Coq, E. Crabb and F. Figueras. J. Mol. Catal., 96 (1995).
[8] B. Coq, A. Bittar, R. Dutrarte and F. Figueras, J. Catal., 128 (1991) 275.
[9] S. Calvagno, A. Donato, G. Neri and R. Pietropaolo, Catal. Lett., 8 (1991) 9
[10] D.C. Koningsberger and R. Prins, X-Ray Absorption: Principles, Applications, Techniques of EXAFS, SEXAFS and XANES, John Wiley and Sons, New York, 1986.
[11] G. Vlaic, J.C.J. Bart, W. Cavigiolo, A. Furesi, V. Ragaini, M.G.A. Catania Sabbadini and E. Burattini, J. Catal., 107 (1987) 263.
[12] J.H. Sinfeld, G.H. Via and F.W. Lytle, J. Chem. Phys., 72 (1980) 4832.
[13] A. Goursot, L. Pedocchi and B. Coq, J. Phys. Chem., 98 (1994) 8747.
[14] G. Neri, L. Mercadante, A. Donato, A.M. Visco and S. Galvagno, Catal. Lett., in press.
[15] J.P. Boiteaux, J. Cosyns and S. Vasudevan, Stud. Surf. Sci. Catal., 16 (1982) 123.
[16] J.J. Rehr, J. Mustre de Leon, S.I. Zabinssky and R.C. Albers, J. Am. Chem. Soc., 113 (1991) 5135.
[17] Appendix of the reports of the International Workshop on Standards and Criteria in Absorption X-ray Spectroscopy, March 7–9, 1988 Brookhaven National Laboratory, Physica B, 158 (1989) 701–722.